Space- and time-resolved spectrophotometry in microsystems

Nicolae Damean, Samuel K. Sia, Vincent Linder, Max Narovlyansky, and George M. Whitesides*

Department of Chemistry and Chemical Biology, Harvard University, 12 Oxford Street, Cambridge, MA 02138

Contributed by George M. Whitesides, June 6, 2005

This work describes a simple optical method for obtaining, in a single still-capture image, the continuous absorbance spectra of samples at multiple locations of microsystems. This technique uses an unmodified bright-field microscope, an array of microlenses, and a diffraction grating to disperse the light transmitted by samples of 10- to 500-μm dimensions. By analyzing in a single image the first-order diffracted light, it is possible to collect the full and continuous absorbance spectra of samples at multiple locations (to a spatial resolution of $\approx$8 μm) in microwells and microchannels to examine dynamic chemical events (to a time resolution of <10 ms). This article also discusses the optical basis of this method. The simultaneous resolution of wavelength, time, and space at a scale <10 μm provides additional capabilities for chemical and biological analysis.

poly(dimethylsiloxane) | array of microlenses | spectrophotometer | image processing

This article describes an optical method that resolves wavelength, time, and location simultaneously for samples in microsystems. This technique, which we call micropattern spectrophotometry (μPS), analyzes a continuous spectrum of wavelengths (with best performance, in the system described here, in the range of 450 to 700 nm) at multiple positions in the field of view of a microscope. This procedure provides a flexible method for analyzing the composition of samples at a number of points, or in a number of samples, simultaneously and continuously.

Microsystems are now ubiquitous in chemistry and biology (1). Applications include analysis of chemical reactions (2), sorting of cells (3), and high-throughput screening (4). Because these systems often require separation (5), mixing (6, 7), and reaction (8) of components with distinct optical profiles, they would benefit from a method that allows the components to be characterized optically in space and time. Advances in miniaturization of components used in spectrophotometric systems have produced a number of useful microsystems: these systems typically work at a single wavelength at any one time (9, 10) or perform measurements at a single spatial location (11–15), and most cannot be easily interfaced with microfluidic systems (16–18). Miniaturized systems for integrating microspectrometers and microfluidics have been proposed but not demonstrated (19, 20). Although fiber optic-based microspectrophotometers (21) have been described and microscope-based spectrophotometers (22) are available, they are capable of analyzing only one or only a few samples at a time, and they scan the spectrum one wavelength at a time. Also, they require alignment of a fiber optic cable to the sample region.

The method described here collects spectral information at many wavelengths and for many samples simultaneously.

Materials and Methods

Setup of the Micropattern Spectrophotometer. We fabricated an array of microlenses in an opaque background by reflowing photoresist (with an index of refraction of 1.59) followed by electroplating of nickel around the microlenses (23–26). We constructed the sample chamber from poly(dimethylsiloxane) (which is optically transparent) by using soft lithography (27, 28). We used a commercially available transmission grating, made of an index-matched epoxy on glass, (92 grooves per mm; Edmund Industrial Optics, Barrington, NJ) in which the pitch was sufficiently small (11 μm) to disperse different wavelengths of visible light into resolvable spatial positions. According to the manufacturer's specifications, the distribution of light at 632 nm through this grating is 45% for 0 order and 20% for -1 and for $+1$ orders.

A Leica (Vienna) DMRX optical microscope served both as light source and detector. The microscope was operated in the transmission mode by using a L $\times$40/0.60 D Plan ∞/0 objective lens (Leitz). A tungsten-halogen lamp acted as the light source, and a black-and-white charge-coupled device (CCD) camera (Hamamatsu ORCA-ER, Hamamatsu Photonics, Hamamatsu City, Japan), which typically has higher sensitivity than color cameras, captured the image containing the diffraction spectra. The time resolution of this experiment was determined by the acquisition time, which was 1–10 ms (depending on the level of illumination of the light source). The images collected by this camera were analyzed with the METAMORPH software package (Universal Imaging, Downingtown, PA). For clarity of visualization, we also captured images with a color camera (Nikon Digital Camera DXM1200).

We characterized the spectral resolving power of the system by using two lasers for the light source rather than broad-spectrum light from the microscope. Onto the stage of the microscope, we placed a glass slide containing the cylindrical microlens, on top of which we placed a transmission grating with the grooves oriented along the long axis of the microlenses. We changed the focus of the objective lens until we observed a clear image of the diffraction spectra and captured an image with the black-and-white CCD camera.

Further details are given in *Supporting Text*, which is published as supporting information on the PNAS web site.

Spectral Measurements Using the Micropattern Spectrophotometer. We obtained quantitative absorbance values of samples over a range of visible wavelengths by analyzing the first-order diffracted light. To measure the absorbance spectrum of a given location of the sample in the field of view, we measured the pixel intensities along a line placed orthogonal to the corresponding diffraction spectrum and converted them to absorbance values as a function of wavelength. To obtain absorbance values of acceptable signal-to-noise, we used lines of 8-μm thickness, which determined the spatial resolution of the method. We used another sample as a standard for calibration to convert the pixels of the camera image to wavelength in nm.

Further details are given in *Supporting Text*.

Results and Discussion

Design of the Micropattern Spectrophotometer. The technique we describe here combines an array of convex microlenses, which

Abbreviations: μPS, micropattern spectrophotometry; CCD, charge-coupled device.

*To whom correspondence should be addressed. E-mail: gwhitesides@gmwgroup.harvard.edu.

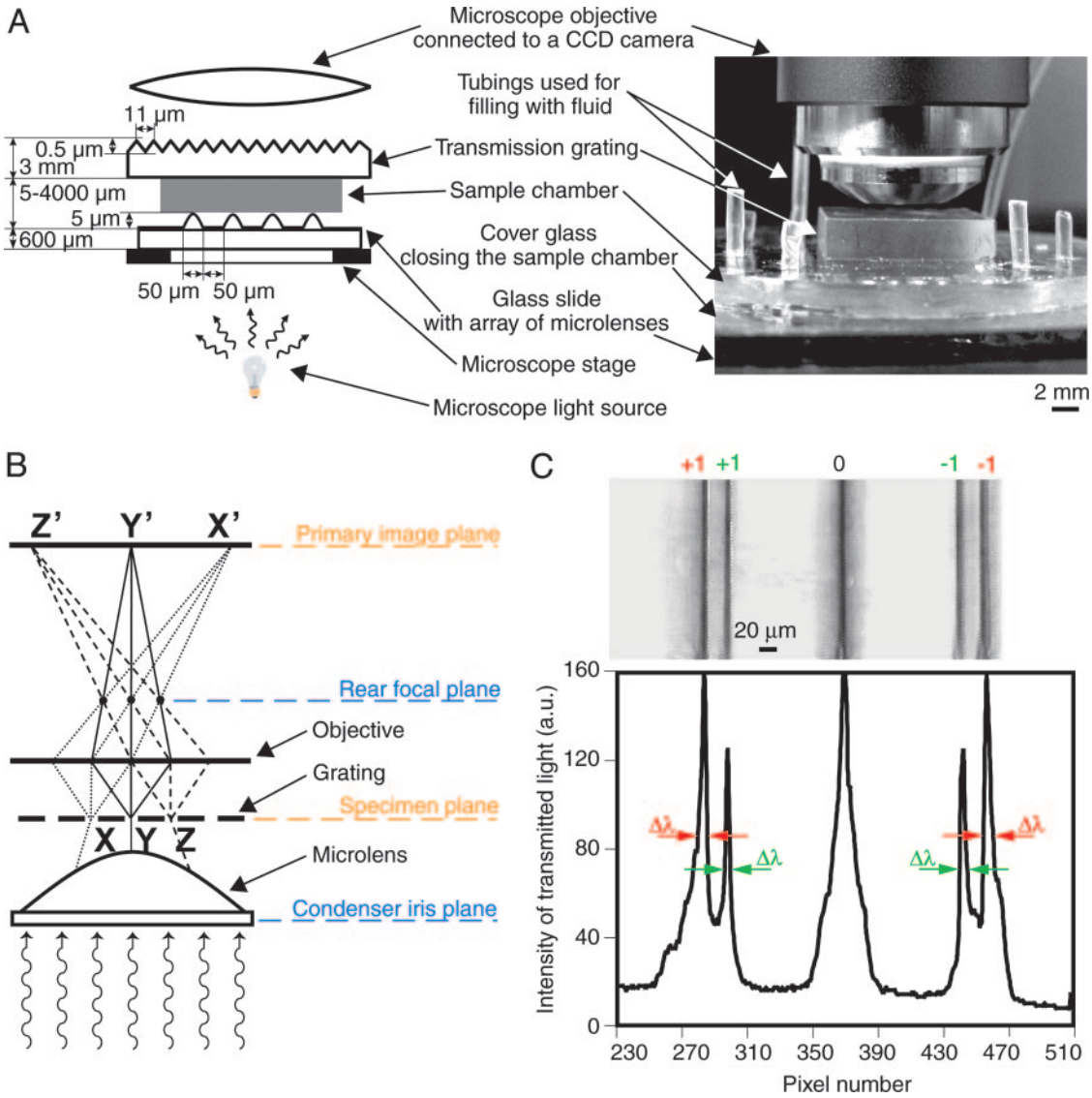

Fig. 1. Setup of μPS. (*A*) Schematic diagram and photograph of the setup. (*B*) Illumination pathway of the optical setup in this study that leads to facile imaging of the diffraction spectrum by using a bright-field microscope. In a regular arrangement for observing diffraction in a microscope, the objective lens is focused on the grating; as a result, an image of the grating forms at the primary image plane (and can be observed via the eyepiece), and an image of the diffracted light forms at the rear focal plane of the objective lens (and can be observed by using a Bertrand lens). In this study, we removed the condenser of the microscope from the light path and used the microlenses as minicondensers. By focusing the objective lens near the microlenses rather than the grating, the optical plane of the condenser iris (which is conjugate to the rear focal plane; both conjugate planes are shown in blue) becomes nearly coplanar with the specimen plane (which is conjugate to the primary image plane; both conjugate planes are shown in orange). As a result, the image of the diffracted light, which is normally observed only in the rear focal plane, also forms on the primary image plane, and is easily captured by a black-and-white CCD camera in a bright-field microscope. (*C*) Determination of spectral resolution using lasers. (*Upper*) In the optical image of the diffraction spectrum, numbers correspond to the diffracted orders, and colors correspond to the wavelengths. (*Lower*) In the processed spectrum of intensity vs. pixel number, the arrows point to the full-width half-maxima that were measured as $\Delta\lambda$, and used to calculate *R*; the colors correspond to the wavelengths.

concentrate light on specific points in the sample, with a transmission grating, which disperses the light that leaves the sample into a continuous spectrum (Fig. 1*A*). The focal distance of the microlenses, as calculated from the equation in ref. 24, is 179 μm. The lenses concentrate the light into the sample placed directly above them. In addition, because the grating is $\approx$3 mm above the sample, well past the focal point of the microlenses, the microlenses help to spread the light at the grating to illuminate a large number of grooves and hence increase the resolution of the diffracted light.

By focusing the objective lens near the microlenses, we capture the diffraction spectrum in the primary image plane; the diffraction spectrum is normally observed only at the rear focal plane (and its conjugate planes) (Fig. 1*B*). Our system has significant advantages over previous methods for observing diffracted light in a microscope (such as using a Bertrand lens): it produces magnified and high-quality images of the diffracted light that are suitable for data processing (compared to low-magnification and spherically distorted images by direct observation of the rear focal plane), and it uses only a bright-field microscope with no requirements for special optics. By analyzing the intensity at each pixel of the image of the first-order diffracted light, and converting the pixel number to wavelength, we easily obtain, for any given spatial position of the sample, the absorbance of the sample vs. wavelength in the visible spectrum.

The sample is normally placed between the microlenses and

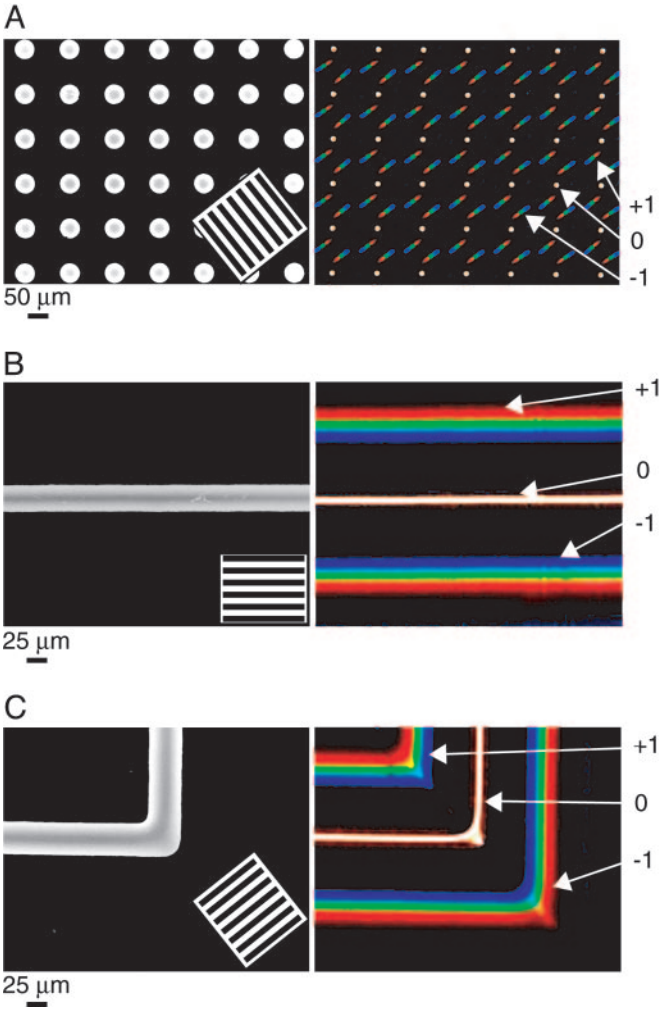

Fig. 2. Diffraction patterns generated by μPS. (*A*) Optical micrograph of an array of spherical microlenses (50 μm in diameter, spaced at 100-μm pitch) (*Left*), a schematic of a transmission grating (92 grooves per mm; the grooves are not drawn to scale for clarity) (*Left Inset*), and a recorded image of the diffraction spectra (*Right*). The diagrams show the orientation of the transmission grating with respect to the microlens. For clarity of visualization, a color CCD camera was used to image the spectra, and no sample chamber was used (such that the diffraction grating lay directly on top of the microlenses). Three orders of diffraction (0, 1, and −1) are visible for each microlens. The image was taken with an objective lens of ×20 magnification. (*B*) As with *A*, but with a straight cylindrical microlens. (*C*) As with *A*, but with a cylindrical microlens with a right-angle turn. The images in *B* and *C* were taken with an objective lens of ×40 magnification.

the grating; this arrangement allows for precise alignment of the microlenses to specific locations of the sample, and thus is useful for analysis of samples in microwells or microchannels where such spatial control is needed. For calibration, where samples (such as optical filters) are homogeneous across the entire field of view, the sample can be placed between the light source and the microlenses, or between the grating and the objective lens.

Determination of the Spectral Resolving Power of the Micropattern Spectrophotometer Using Lasers. Using the formula of spectral resolving power $R = \lambda/\Delta\lambda$, where $\Delta\lambda$ denotes the full-width half-maximum at a particular wavelength λ, we obtained a R of 21 (Fig. 1*C*), which is similar to the spectral resolving power of current industrial integrated optical microspectrometers (11, 15).

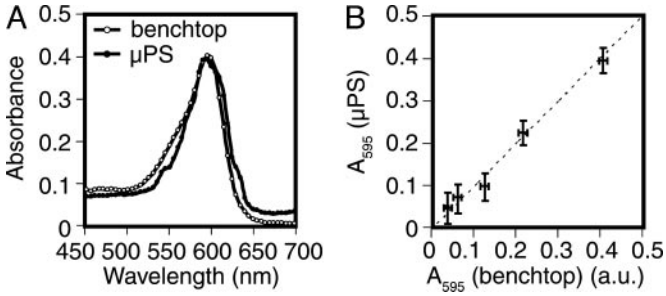

Fig. 3. Quantitative characterization of μPS. (*A*) Comparison of wavelength spectra of 6.0 mM bromophenol blue as measured by μPS and a benchtop spectrophotometer. (*B*) Comparison of absorbance values measured by μPS and a benchtop spectrophotometer, for different concentrations of bromophenol blue (from 0.4 to 6.0 mM). The absorbance values were measured at 595 nm, the absorption maximum of bromophenol blue.

Using Different Patterns and Geometries of Microlenses in the Micropattern Spectrophotometer. We next analyzed the diffraction spectra that resulted from a number of different patterns and geometries of microlenses. An array of spherical microlenses, combined with a transmission grating, generated an array of discrete spots (corresponding to the zeroth order of diffraction, or light that passed straight through the grating) with two accompanying diffraction spectra (corresponding to the +1 and −1 orders of diffracted light) (Fig. 2*A*); the grating used in this study does not efficiently produce higher orders of diffracted light, and therefore avoids the overcrowding of diffraction spectra. As expected, blue light diffracted to a lesser extent than red light, with an observed linear dispersion of 0.4 μm/nm in the first-order diffracted light. Overall, the pattern of diffracted light demonstrates that an array of spherical microlenses is useful for obtaining visible spectra at multiple discrete locations of a sample in a microsystem, such as microwells and microarrays, and for analyzing the same sample at multiple locations for signal averaging.

The pattern of diffracted light that was generated by a cylindrical microlens and a transmission grating shows that the +1 and −1 orders of diffracted light are manifested as continuous lines (Fig. 2*B*). Moreover, for a cylindrical microlens that turns at a right angle, the grating can be oriented at 45° to each segment of the microlens to produce a continuous set of spectra for both segments (Fig. 2*C*). Thus, the pattern of diffracted light suggests that cylindrical microlenses are useful for measuring a continuous set of spectra for samples in microfluidic systems with a variety of geometries of microchannels.

Comparison Between Micropattern Spectrophotometer and Benchtop Spectrophotometer. We extracted quantitative absorbance values of samples constituted from dilutions of bromophenol blue over a range of visible wavelengths. A dye in a quartz cuvette served as the sample. Using another dye as a standard for calibration we converted the pixels of the camera image to wavelength in nm. This methodology is detailed in Figs. 6–8, which are published as supporting information on the PNAS web site.

Over the 450- to 700-nm range, the absorbance values measured by μPS for dilutions of bromophenol blue show good agreement with those obtained by a benchtop spectrophotometer, with the average difference between these two sets of data being 0.02 arbitrary units for a sample of 6 mM of bromophenol blue (Fig. 3*A*). From Fig. 6*C*, the absorbance maximum of bromophenol blue was measured to be 595 nm, whereas the benchtop spectrophotometer showed that the absorbance maximum was 599 nm. Thus, we resolved the absorbance maximum to an error of 4 nm, or ≈3 pixels. At the absorption maximum, μPS yielded absorbance values that closely matched those ob-

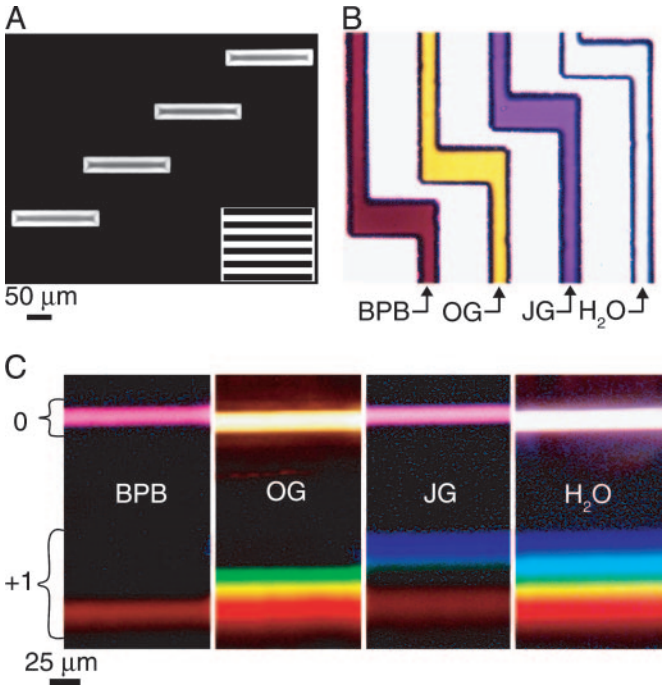

Fig. 4. Use of μPS to measure simultaneously the visual spectra of dyes in multiple microwells. (*A*) Optical micrograph of an array of cylindrical microlenses, and a schematic of transmission grating (with its orientation with respect to the microlenses) (*Inset*). (*B*) Optical micrograph of a system of four microwells (90 μm deep) filled with dyes. For the four microwells, from left to right, the dyes are bromophenol blue (BPB), orange green (OG), Janus green (JG), and MQ water as a blank. (*C*) Recorded images of the diffracted spectra (only 0 and +1 orders are shown) with a color CCD camera.

tained by the benchtop spectrophotometer over a range of dilutions of bromophenol blue, with an average absolute deviation between the two methods of 0.03 absorbance units (Fig. 3*B*). The dashed line in Fig. 3*B* corresponds to an ideal correlation: that is, one in which both instruments yield the same value of absorbance for every dilution. The main factor that contributed to the average absolute deviation between the two sets of experimental results was given by the procedure of calibration.

Use of the Micropattern Spectrophotometer for Spectral Measurements in Microwells. To demonstrate the use of μPS in microsystems, we measured the wavelength spectra of different dyes in a set of microwells by analyzing their diffracted light. In this experiment, we used a set of 50-μm-wide cylindrical microlenses (Fig. 4*A*) and fabricated four 90-μm-deep and 100-μm-wide microwells in a poly(dimethylsiloxane) microchip by soft lithography (27, 28), to which we added different dyes, and MQ water as a blank, through 50-μm-wide microchannels (Fig. 4*B*). After aligning the microlenses to the microwells, and placing the grating on the sample chamber so that the grooves were parallel to the long axis of the microlenses (Fig. 4*A*), we recorded the four diffraction spectra on one image with a black-and-white CCD camera. For clarity of visualization, we also captured images of the diffraction spectra with a color camera (Fig. 4*C*).

Analysis of the pixel intensities of the first-order diffracted light, followed by conversion of pixel number to wavelengths, revealed absorbance maxima of 626, 436, and 601 nm (with an error of ±9 nm) for bromophenol blue, orange green, and Janus green, respectively. The values expected from measurements with a benchtop spectrophotometer are 610, 448, and 575 nm. One factor that contributed to the average absolute deviation between the two sets of experimental results was the referencing

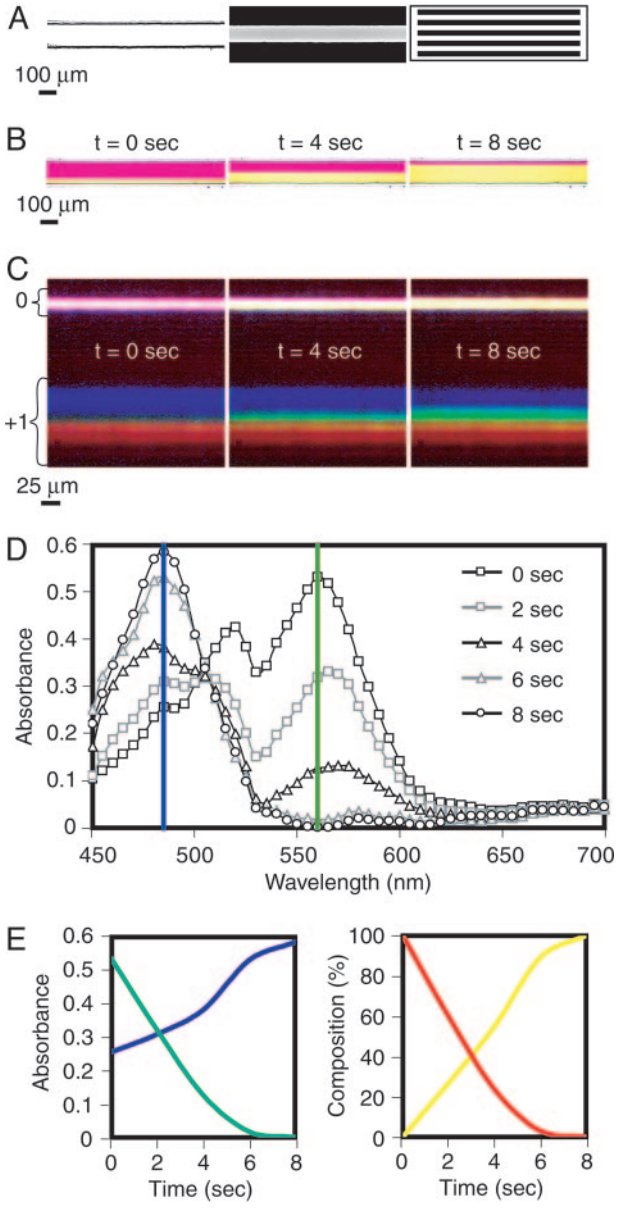

Fig. 5. Monitoring of dynamic events in a laminar flow experiment using μPS. (*A*) Optical micrographs of a microchannel (*Left*) and a microlens aligned to the microchannel (*Center*), and a schematic diagram of a transmission grating (*Right*) with the grooves parallel to the microchannel. (*B*) Optical micrographs of laminar flow of fluorescein and sulforhodamine B in a microchannel. (*C*) Images of the diffraction spectra with different compositions of dyes in the microchannel (which can be roughly observed in the zeroth-order spectra). The zeroth- and first-order diffracted spectra are shown. For clarity of visualization, color images are shown. (*D*) Absorbance spectra of a specific location in the microchannel, as a change in flow rates fills a microchannel primarily with sulforhodamine B to one filled primarily with fluorescein, over the course of 8 s. (*E*) (*Left*) The absorbance values recorded at 485 nm (blue) and 560 nm (green) over the course of the switching of flow rates. (*Right*) The percentage composition of fluorescein (yellow) and sulforhodamine B (red) in the microchannel during the experiment.

of data to a blank in a different microwell (for example, MQ water in one channel served as the blank for a sample in a different channel). In addition, nonuniform contacts between the sample chamber and optical components (i.e., microlenses and transmission grating), as well as roughness (at the μm scale) of the surface of the microchannels, can scatter the light.

Spectral Measurements of Dyes in Dynamic Events. We built a system to monitor the dynamic switching of dye-containing fluid streams in laminar flow. A straight cylindrical lens was aligned to the center of a microchannel (Fig. 5*A*), in which fluorescein and sulforhodamine B flow side by side. We changed the composition of the fluid in the microchannel by varying the flow rate of each dye (Fig. 5*B*). By capturing images of the diffraction spectra (Fig. 5*C*) while varying the flow rates, the full absorbance spectra of an arbitrary location in the microchannel were measured over time (Fig. 5*D*). Processing of the data showed the dynamic changes in the composition of fluids in the channel over 8 s (Fig. 5*E*). Although we captured images every 0.4 s in this experiment, the time resolution of the system is limited by the acquisition time of the CCD camera, which can be as low as 1–10 ms.

Conclusions

This work demonstrates a versatile technique for analyzing the visible spectra in microsystems. This technique integrates readily available equipment (an optical microscope and a CCD camera) with inexpensive optical components (an array of microlenses and a transmission grating) into a single system that extends the applicability of microsystems. It provides a practical capability to the rapidly growing field of microanalysis, including microfluidic applications, microarray and high-throughput experiments, and analysis of samples with microscale optical variations [such as patterned surfaces of biological molecules (27), thin films of polymers (29), liquid crystals (30), metals, and semiconductors]. By dispersing wavelengths reproducibly, it allows an inexpensive black-and-white CCD focal plane array to provide information at multiple wavelengths, and at multiple locations, in a single image. Disadvantages of the method include: use in the visible spectrum only (although the range of wavelengths can in principle be extended with appropriate optics), and lower spectral resolution and sensitivity than the benchtop spectrophotomer. The thickness of the sample chamber and the vertical dimension of the micropattern spectrophotometer are limited by the working distance of the microscope objective, which in our case was 7.1 mm.

We thank Richard Conroy and Dmitri V. Vezenov for helpful discussions on the optics of this study. This work was supported by National Institutes of Health Grant GM065364 and a Defense Advanced Research Planning Agency subaward from the California Institute of Technology. S.K.S. was supported by a Canadian Institutes of Health Research Fellowship. V.L. was supported by a postdoctoral fellowship from the Swiss National Foundation.

1. Vilkner, T., Janasek, D. & Manz, A. (2004) *Anal. Chem.* **76,** 3373–3386.
2. Losey, M. W., Schmidt, M. A. & Jensen, K. F. (2001) *Ind. Eng. Chem. Res.* **40,** 2555–2562.
3. Chou, H., Spence, C., Scherer, A. & Quake, S. R. (1999) *Proc. Natl. Acad. Sci. USA* **96,** 11–13.
4. Dunn, D. A. & Feygin, I. (2000) *Drug Discovery Today* **5,** S84–S91.
5. Huang, L. R., Cox, E. C., Austin, R. H. & Sturm, J. C. (2004) *Science* **304,** 987–990.
6. Ottino, J. M. & Wiggins, S. (2004) *Science* **305,** 485–486.
7. Song, H. & Ismagilov, R. F. (2003) *J. Am. Chem. Soc.* **125,** 14613–14619.
8. Kamholz, A. E., Weigl, B. H., Finlayson, B. A. & Yager, P. (1999) *Anal. Chem.* **71,** 5340–5347.
9. Adams, M. L., Enzelberger, M., Quake, S. R. & Scherer, A. (2003) *Sens. Actuators A* **104,** 25–31.
10. Sato, Y., Irisawa, G., Ishizuka, M., Hishida, K. & Maeda, M. (2003) *Meas. Sci. Technol.* **14,** 114–121.
11. Yee, G. M., Maluf, N. I., Hing, P. A., Albin, M. & Kovacs, G. T. A. (1997) *Sens. Actuators A* **58,** 61–66.
12. Wendt, J. R., Warren, M. E., Sweatt, W. C., Bailey, C. G., Matzke, C. M., Arnold, D. W., Allerman, A. A., Carter, T. R., Asbill, R. E. & Samora, S. (1999) *J. Vac. Sci. Technol. B* **17,** 3252–3255.
13. Workman, J., Jr., Koch, M. & Veltkamp, D. J. (2003) *Anal. Chem.* **75,** 2859–2876.
14. Hulme, J. P., Mohr, S., Goddard, N. J. & Fielden, P. R. (2002) *Lab Chip* **2,** 203–206.
15. Wolffenbuttel, R. F. (2004) *IEEE Trans. Instrum. Meas.* **53,** 197–202.
16. Roulet, J.-C., Völkel, R., Herzig, H. P., Verpoorte, E., de Rooij, N. F. & Dändliker, R. (2001) *J. Microelectromech. Syst.* **10,** 482–491.
17. Roulet, J.-C., Völkel, R., Herzig, H. P., Verpoorte, E., de Rooij, N. F. & Dändliker, R. J. (2001) *Opt. Eng.* **40,** 814–821.
18. Simpson, M. L., Dress, W. B., Ericson, M. N., Jellison, G. E., Sitter, D. N., Wintenberg, A. L. & Frenchet, D. F. (1998) *Rev. Sci. Instrum.* **69,** 377–383.
19. Traut, S. & Herzig, H. P. (2000) *Opt. Eng.* **39,** 290–298.
20. Verpoorte, E. (2003) *Lab Chip* **3**, 42N–52N.
21. Ocean Optics (2004) *Spectrometers and Accessories Catalog* (Ocean Optics, Dunedin, FL).
22. CRAIC Technologies (2004) *UV-Visible-NIR Microspectrometers Catalog* (CRAIC Technologies, Altadena, CA).
23. Wu, M. & Whitesides, G. M. (2002) *J. Micromech. Microeng.* **12,** 747–758.
24. Wu, H. & Whitesides, G. M. (2002) *Anal. Chem.* **74,** 3267–3273.
25. Nussbaum, P. & Herzig, H. P. (2001) *Opt. Eng.* **40,** 1412–1414.
26. Schilling, A., Merz, R., Ossmann, C. & Herzig, H. P. (2000) *Opt. Eng.* **39,** 2171–2176.
27. Whitesides, G. M., Ostuni, E., Takayama, S., Jiang, X. Y. & Ingber, D. E. (2001) *Annu. Rev. Biomed. Eng.* **3,** 335–373.
28. Sia, S. K. & Whitesides, G. M. (2003) *Electrophoresis* **24,** 3563–3576.
29. Steckman, G. J., Shelkovnikov, V., Berezhnaya, V., Gerasimova, T., Solomatine, I. & Psaltis, D. (2000) *Opt. Lett.* **25,** 607–609.
30. Wang, Y. Z., Run, R. G., Wang, D. K., Swager, T. M. & Epstein, A. J. (1999) *Appl. Phys. Lett.* **74,** 2593–2595.